Front. Med. 2020, 14(3): 305–317
https://doi.org/10.1007/s11684-019-0722-8

RESEARCH ARTICLE

Keratin 5-Cre-driven deletion of *Ncstn* in an acne inversa-like mouse model leads to a markedly increased IL-36a and Sprr2 expression

Jun Yang[1,*], Lianqing Wang[1,2,*], Yingzhi Huang[1], Keqiang Liu[1], Chaoxia Lu[1], Nuo Si[1], Rongrong Wang[1], Yaping Liu (✉)[1], Xue Zhang (✉)[1]

[1]*McKusick-Zhang Center for Genetic Medicine, State Key Laboratory of Medical Molecular Biology, Institute of Basic Medical Sciences Chinese Academy of Medical Sciences, School of Basic Medicine Peking Union Medical College, Beijing 100005, China;* [2]*Center of Translational Medicine, Central Hospital of Zibo, Shandong University, Zibo 255036, China*

Abstract **Familial acne inversa (AI) is an autoinflammatory disorder that affects hair follicles and is caused by loss-of-function mutations in γ-secretase component genes. We and other researchers showed that *nicastrin* (*NCSTN*) is the most frequently mutated gene in familial AI. In this study, we generated a keratin 5-Cre-driven epidermis-specific *Ncstn* conditional knockout mutant in mice. We determined that this mutant recapitulated the major phenotypes of AI, including hyperkeratosis of hair follicles and inflammation. In *Ncstn*$^{flox/flox}$;*K5-Cre* mice, the IL-36a expression level markedly increased starting from postnatal day 0 (P0), and this increase occurred much earlier than those of TNF-α, IL-23A, IL-1β, and TLR4. RNA-Seq analysis indicated that Sprr2d, a member of the small proline-rich protein 2 family, in the skin tissues of the *Ncstn*$^{flox/flox}$;*K5-Cre* mice was also upregulated on P0. Quantitative reverse-transcription polymerase chain reaction showed that other *Sprr2* genes had a similar expression pattern. Our findings suggested that IL-36a might be a key inflammatory cytokine in the pathophysiology of AI and implicate malfunction of the skin barrier in the pathogenesis of AI.**

Keywords acne inversa mouse model; interleukin 1 family, member 6; small proline rich protein 2D; key inflammatory cytokine

Introduction

Acne inversa (AI), also referred to as hidradenitis suppurativa, is a chronic and recurrent inflammatory disease affecting hair follicles and characterized by abscesses, sinus tracts, and scar formation [1]. In AI, lesions occur abundantly in areas where large sweat glands are distributed. The exact prevalence of AI is unknown, but it has an estimated overall prevalence of 0.1% in the United States [2] and 1% in Europe [3–5]. The potential risk factors of AI include smoking and obesity [6,7], and the possible contributors of this disease are immune responses and bacterial infection [8]. The onset of AI is usually after puberty, and the disease has been regarded as androgen dependent [9]. Therefore, sex hormones are considered to be cofactors in AI. Approximately 30% – 40% of affected patients have a family history of AI that typically presents with an inheritance pattern of autosomal dominance and is associated with genetic heterogeneity [10,11]. Studies have also shown the reduced penetrance in AI [6,12].

The causal genes of familial AI, namely, *PSEN1*, *NCSTN*, and *PSENEN*, which are the encoding components of γ-secretase, were identified in 2010 [13]. Subsequent studies have shown that *NCSTN* is the major gene mutated in familial AI. γ-Secretase functions as a transmembrane protease involved in the Notch signaling pathway. The haploinsufficiency of γ-secretase leads to an impaired downstream functioning of the Notch pathway, and this impairment is considered a possible cause of AI [14]. However, the pathogenesis of AI is not fully understood.

The occurrence and development of AI are possibly due

Received May 16, 2019; accepted September 7, 2019

Correspondence: Yaping Liu, ypliu@ibms.pumc.edu.cn;
Xue Zhang, xuezhang@pumc.edu.cn

*The authors contributed equally to this work.

to hyperkeratosis of hair follicles, leading to the occlusion and rupture of the pilosebaceous unit [15]. In this process, exogenous bacteria and cortical keratinocytes are released into the dermis, immune function is dysregulated, and inflammatory cells infiltrate the affected area [16]. The overexpression of proinflammatory cytokines in this disease and the therapeutic efficacy of cytokine inhibitors highlight the important roles of inflammatory cytokines in the pathogenesis of AI [17,18]. The inhibition of tumor necrosis factor-α (TNF-α) likely improves the condition of patients with AI [19,20]. Interleukin (IL)-1 and IL-23 inhibitors have also been shown to result in favorable outcomes in AI [21]. Kelly *et al*. [22] suggested that immune dysregulation acts critically in initiating and propagating AI in the skin of patients. These lines of evidence support the hypothesis that inflammatory cytokines are the major contributors to the pathogenesis of AI.

The products of *SPRR2* are members of the small proline-rich protein 2 family. This family provides barrier functions in stratified squamous epithelial cells, thereby protecting against environmental damage. These proteins are also involved in inflammatory skin diseases [23].

In the present study, we established a conditional *Ncstn* knockout mouse model in which AI-like phenotypes were recapitulated. Herein, we described our findings on alterations in gene expression *in vivo* and *in vitro* and emphasized the important roles of IL-36a and Sprr2 in the pathogenesis of AI.

Materials and methods

Animal model construction

Ncstn$^{flox/flox}$ mice were purchased from Jackson Laboratory (Bar Harbor, ME, USA), and *K5-Cre* mice were provided by Professor Xiao Yang (State Key Laboratory of Proteomics, Genetic Laboratory of Development and Diseases, Institute of Biotechnology, Beijing, China). These strains were mated to yield heterozygous knockout *Ncstn* (*Ncstn*$^{flox/+}$;*K5-Cre*) mice. The *Ncstn*$^{flox/+}$;*K5-Cre* and *Ncstn* (*Ncstn*$^{flox/flox}$) mice were mated to generate a keratinocyte-specific null mutant of *Ncstn* (*Ncstn*$^{flox/flox}$;*K5-Cre*) in mice through the Cre-loxP system. All mouse models were kept in a specific pathogen-free environment.

Hematoxylin and eosin staining

Paraffin-embedded sections (3 μm) were heated at 56 °C for 30 min and treated with xylene twice for 20 min each. Slides were dehydrated by rinsing with 100% ethanol twice for 5 min each, graded ethanol, and distilled water. Afterward, the tissue sections were deparaffinized, rehydrated, and stained with hematoxylin for 20 min and with eosin for 5 min. Subsequently, the slides were rinsed in prespecified concentrations of ethanol, distilled water, and xylene for 5 min each. Stained tissue images were captured with a microscope (Olympus, Tokyo, Japan).

Microarray analysis

The tissues of the back skin of the heterozygous knockout *Ncstn* (*Ncstn*$^{flox/+}$;*K5-Cre*) mice and the null *Ncstn* mutant (*Ncstn*$^{flox/flox}$;*K5-Cre*) mice were obtained at multiple ages (i.e., postnatal days 0 [P0], 10 [P10], 15 [P15], 30 [P30], and 45 [P45]). The gene expression patterns of the 10 resulting samples were ascertained using an Affymetrix GeneChip Mouse Genome 430 2.0 array (Santa Clara, CA, USA) and scanned with Affymetrix GeneChip Command Console. The samples met the predetermined quality criteria, and standard microarray hybridization was performed [24]. The thresholds used to filter upregulated or downregulated genes were $\geqslant$ 1.5-fold changes and $P < 0.05$. Data were screened for differentially expressed genes based on gene ontology (GO) terms, biological pathways, and intersection.

RNA-Seq analysis

The skin tissues obtained from the backs of the *Ncstn*$^{flox/flox}$;*K5-Cre* and control mice on P0 and P30 were collected, and three specimens were prepared as the biological replicates of each genotype. Total RNA was isolated from the skin by using TRIzol reagent (Ambion, Life Technologies, Carlsbad, CA, USA). RNA-Seq was performed by Novogene (Chula Vista, CA, USA) on an Illumina Hiseq 2000/2500 platform. Single-end clean reads were aligned to the reference genome by using TopHat (v2.0.9, Johns Hopkins University, Baltimore, MD, USA). Differential gene expression between the two groups was verified with the DESeq R package (v1.10.1, Bioconductor). Between-group differential gene expression was analyzed using the DEGseq (2010) R package [25,26]. Significantly different expression was defined as $P < 0.005$ and $|\log_2(\text{fold change})| > 5$. The genes were further screened through GO and KEGG enrichment analysis.

RNAi

HaCaT cells were cultured in Eagle's minimum essential medium with Earle's balanced salts (Union Cell Resource Center, Beijing, China), supplemented with 10% fetal bovine serum (Gibco, Carlsbad, CA, USA) and 1% penicillin and streptomycin in a 5% CO_2 incubator at 37 °C. *NCSTN* and *NOTCH1* siRNAs and control siRNAs were synthesized by GenePharma (Shanghai, China; Supplementary Table S4). Lipofectamine 3000 was purchased from Invitrogen (Waltham, MA, USA). HaCaT cells (1×10^5) were seeded in six-well plates and incubated overnight. Afterward, the cells with

30%–50% confluence were treated with 100 pmol of siRNA precomplexed with Lipofectamine 3000 in accordance with the manufacturer's protocol. RNA and protein were extracted 48 and 72 h after siRNA transfection, and expression was quantified through quantitative reverse-transcription polymerase chain reaction (qRT-PCR) and Western blot. Results were depicted as the mean of three independent experiments.

Results

Mouse mutant construction and verification

NCSTN encodes the NCSTN subunit of γ-secretase. Loss-of-function mutations in this gene play a pivotal role in the etiology of AI [27–29]. Keratinocyte-specific *Ncstn*-knockout mice were generated by using the Cre-loxP system. Specifically, a mouse strain that carried loxP sites in flanking exon 3 of *Ncstn* (*Ncstn*$^{flox/flox}$) was mated with transgenic mice expressing Cre under the control of the keratin 5 (*K5*) promoter (Fig. 1A). The *K5* promoter directs gene expression from E13.5 in follicular keratinocytes and in the basal layer of the epidermis; therefore, this strategy enabled the disruption of the floxed *Ncstn* expression throughout the epidermis and the outer root sheaths of hair follicles [30]. The genomic DNA from the toes of the knockout mice was amplified using specific primers to validate the genotype (Fig. 1B and 1C). *K5-Cre* was detected as described previously [31], and *K5-Cre* mice were designated as the control group (WT). All experimental procedures, including qRT-PCR, immunofluorescence staining (IF), and Western blot, were performed to verify whether *Ncstn* was effectively knocked out in the skin tissue of *Ncstn*$^{flox/flox}$*;K5-Cre* mice (Fig. 1D–1G). The Ncstn expression at various hair cycle stages was also measured. Our findings indicated that the expression of this gene did not correlate with hair cycle stages. The mRNA and protein expression levels of *Ncstn* in *Ncstn*$^{flox/flox}$*;K5-Cre* mice decreased significantly, suggesting that the conditional null mutant was generated.

Phenotypic and pathophysiologic characterization of the mouse model

The *Ncstn*$^{flox/flox}$*;K5-Cre* mice were morphologically similar to the WT mice from birth to P15. On approximately P21, the *Ncstn*$^{flox/flox}$*;K5-Cre* mice began shedding hair on the upper eyelid. This shedding extended gradually from the head and face to the back and was accompanied with the hyperkeratosis of the hair follicles. The area of hair loss covered primarily the head, face, and back of the neck. Concurrently, hyperkeratosis developed and spread over the entirety of the skin, and alopecia was observed in the most severely affected areas. The *Ncstn*$^{flox/flox}$*;K5-Cre* mice could not open their eyes in the later stages because of the hyperkeratosis of the eyelids (Fig. 2A). These mice died on approximately P70. However, the heterozygous mutant (*Ncstn*$^{flox/+}$*;K5-Cre*) mice and the WT mice had no obvious deficits.

The majority of AI-causing mutations involve a predicted loss-of-function effect on γ-secretase [32,33]. We performed qRT-PCR and Western blot analysis to examine the expression of Notch1, an immediate substrate of γ-secretase, in the skin tissues of the mutant mice. As shown in Fig. 2C, the mRNA expression of Notch1 in the *Ncstn*$^{flox/flox}$*;K5-Cre* mice was markedly downregulated compared with that in the WT mice. Western blot findings indicated a very weak signal corresponding to the intracellular domain of Notch1 (Fig. 2D and 2E), confirming that the enzymatic cleavage activity of γ-secretase was lost in the mutant group.

To further investigate pathophysiologic features in the model of AI, we performed hematoxylin and eosin staining on the skin specimens of the mutant and WT mice on P15, P30, and P45. On P15, the number and shape of the hair follicles of the *Ncstn*$^{flox/flox}$*;K5-Cre* and WT mice were similar (Fig. 2B). On P30, the *Ncstn*$^{flox/flox}$*;K5-Cre* mice showed loss of the fat layer because of the excessive hyperplasia of keratinocytes. Nevertheless, the mutant mice retained normal-appearing hair follicles at this stage, and a few keratotic plugs were observed. On P45, the hair follicles of the *Ncstn*$^{flox/flox}$*;K5-Cre* mice were found to be severely atrophic and further keratinized, and many keratotic plugs were observed. In addition, the skin was markedly thickened, and hair follicle cycling was lost (Fig. 2B).

AI is an autoinflammatory disorder affecting hair follicles and involving multiple inflammatory cytokines that participate in immune dysregulation. We detected the expression of TLR4 and three well-known inflammatory cytokines, namely, TNF-α, IL-23A, and IL-1β, and found that their expression levels significantly increased (Fig. 2F–2I). This finding was consistent with clinical results. In patients, the onset of AI is characterized by the hyperkeratosis and subsequent blockage of hair follicles, followed by inflammatory reactions and possibly by secondary infections. In our study, the *Ncstn* null mutant mice exhibited hyperkeratosis and inflammation phenotypes similar to those seen in patients with AI. Therefore, we considered the *Ncstn* null mutant mice to be an appropriate model system for studies on AI pathogenesis.

Upregulation of IL-36a and LCN2 in the skin of the mouse model

The skin specimens of the *Ncstn*$^{flox/flox}$*;K5-Cre* and *Ncstn*$^{flox/+}$*;K5-Cre* mice were obtained at five stages (P0, P10, P15, P30, and P45) and analyzed for gene expression. In comparison with the genes of the *Ncstn*$^{flox/+}$*;K5-Cre* mice, 5295 genes were downregulated and 6201 genes

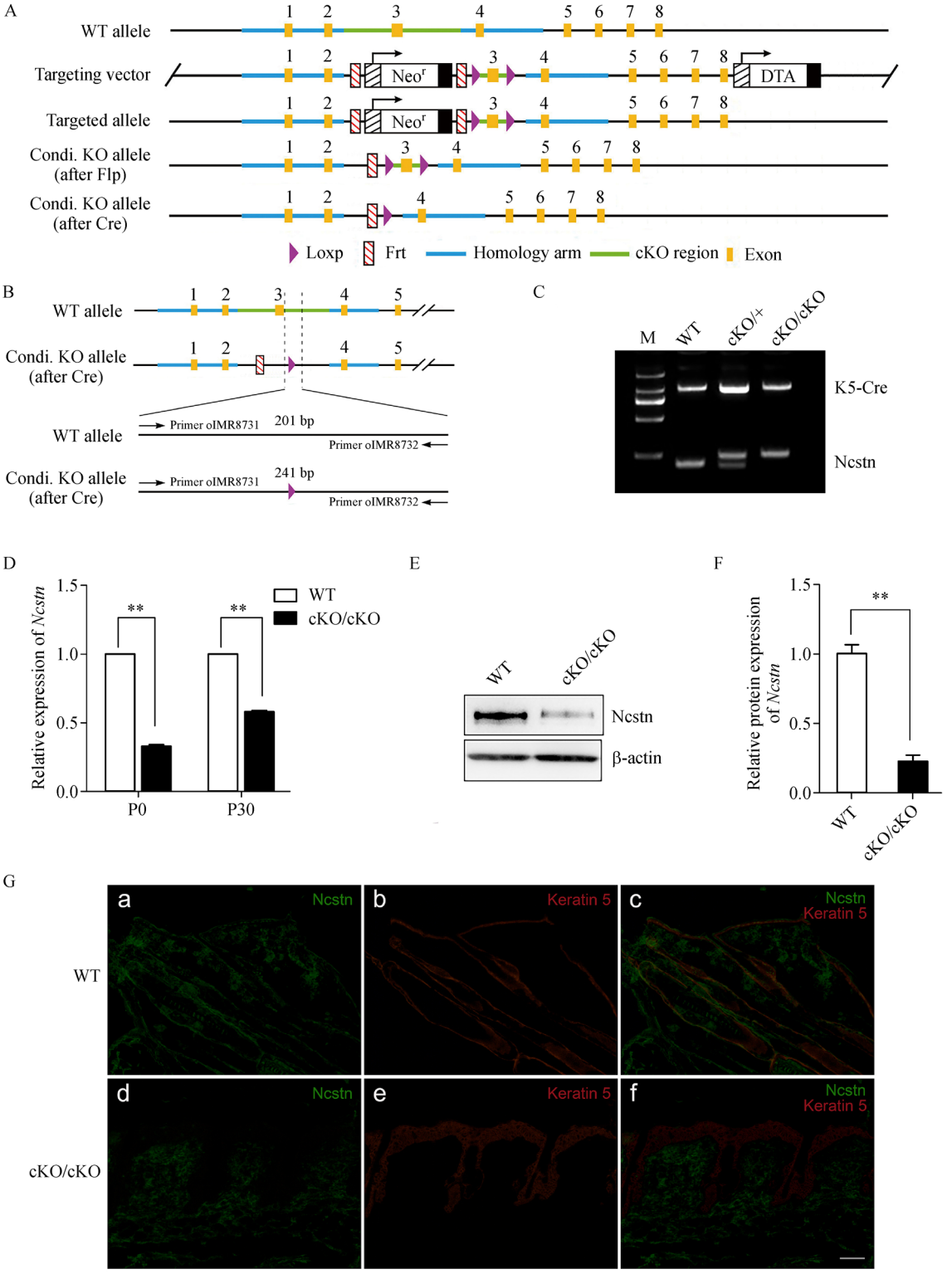

Fig. 1 Mouse mutant construction and verification. (A) Conditional *Ncstn* knockout strategy. (B) Primers used for genotyping the mice. (C) Agarose gel results showing the genotypes of the mice. *K5-Cre* mice were named WT. The cKO/cKO group was *Ncstn*$^{flox/flox}$;*K5-Cre*. The cKO/+ group corresponded to *Ncstn*$^{flox/+}$;*K5-Cre*. M, DNA marker (DL2000). (D) The knockout efficiency of *Ncstn* in the skin of WT and *Ncstn*$^{flox/flox}$;*K5-Cre* mice was determined at the mRNA level on P0 and P30. Data shown were mean ± standard deviation (SD) of three independent experiments, and each experiment was performed in duplicate. Two asterisks denoted $P < 0.01$. The ratio of Ncstn to β-actin in WT mice was set to 1. The (E) presence/absence and (F) quantification level of Ncstn protein in WT and *Ncstn*$^{flox/flox}$;*K5-Cre* mice skin were determined on P30. (G) Immunofluorescence staining results for Ncstn (green) and keratin 5 (red) in the skin of WT (a–c) and *Ncstn*$^{flox/flox}$;*K5-Cre* (d–f) mice on P30. Scale bar = 50 μm.

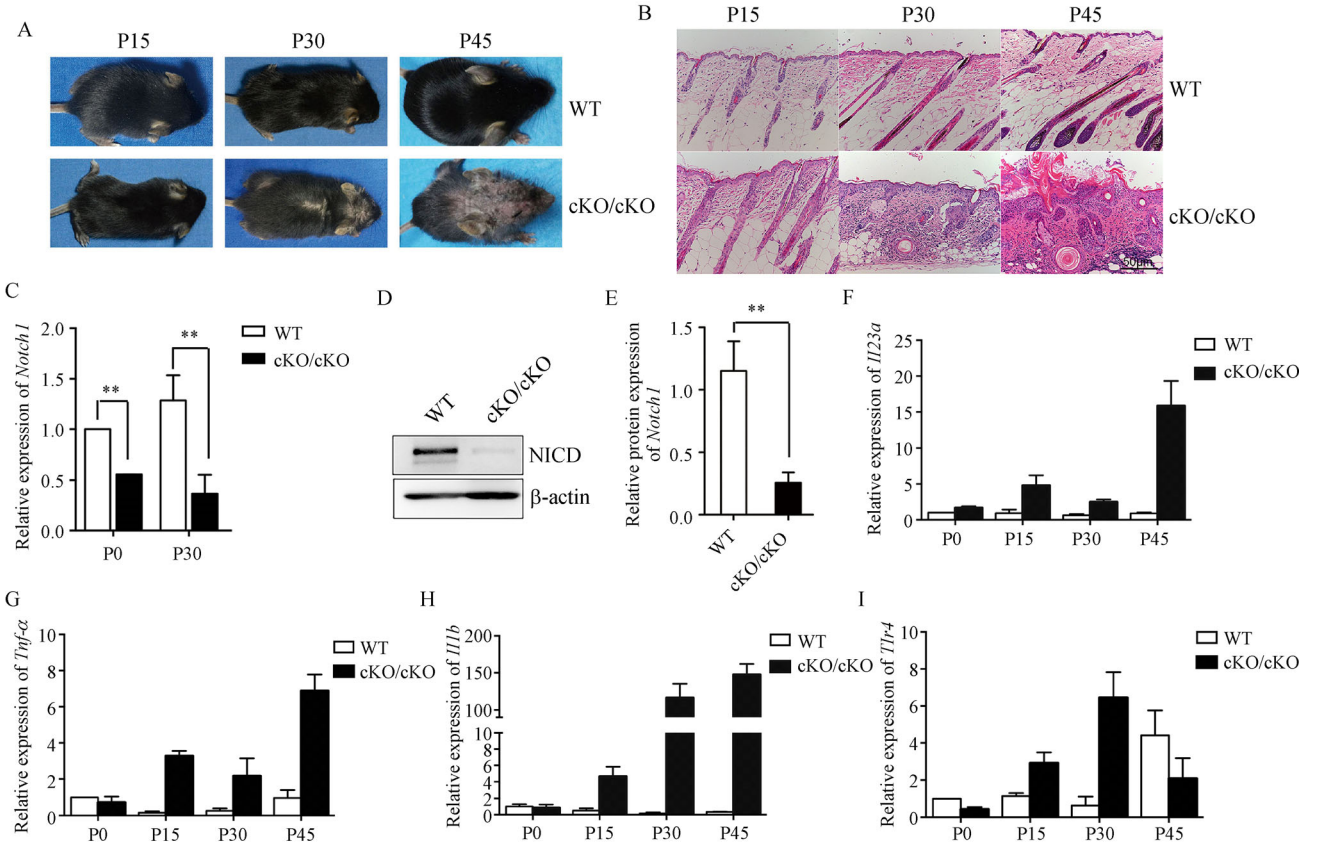

Fig. 2 Phenotypic and pathophysiologic characterization of the mouse model. (A) The skin appearance of *Ncstn*$^{flox/flox}$*;K5-Cre* and WT mice at the indicated postnatal ages. (B) Hematoxylin- and eosin-stained skin sections on P15, P30, and P45. Scale bar = 50 μm. (C) mRNA expression of Notch1 in the skin of WT and *Ncstn*$^{flox/flox}$*;K5-Cre* mice on P0 and P30, ascertained by qRT-PCR. Data shown were mean ± SD of three experiments, and each experiment was performed in duplicate. The ratio of Notch1 to β-actin in WT mice on P0 was set to 1. Two asterisks denoted $P < 0.01$. Western blot was used to determine the (D) presence/absence and (E) quantification level of the cleaved Notch1 (NICD) in the mouse skin. Results of quantitative reverse-transcription polymerase chain reaction for (F) *Il23a*, (G) *Tnf-α*, (H) *Il1b*, and (I) *Tlr4*. Data shown were mean ± SD of three experiments, and each experiment was performed in duplicate. The ratio of the gene of interest to β-actin in WT mice on P0 was set to 1.

were upregulated in the *Ncstn*$^{flox/flox}$*;K5-Cre* mice. The scatter plot and hierarchical clustering map revealed the differential gene expression levels in the *Ncstn*$^{flox/flox}$*;K5-Cre* mice versus the *Ncstn*$^{flox/+}$*;K5-Cre* mice (Fig. 3). All the differentially expressed genes from the five stages were screened to obtain an intersection data set. From this data set, only two probes remained: *Il1f6* (1418609_at) and *Lcn2* (1427747_a_at). These two genes were upregulated in the *Ncstn*$^{flox/flox}$*;K5-Cre* mice at all five stages.

We performed qRT-PCR to validate whether IL-36a and LCN2 expression levels were upregulated in the skin of the *Ncstn*$^{flox/flox}$*;K5-Cre* mice at multiple hair follicle stages. As shown in Fig. 4A and 4C, the mRNA expression levels of IL-36a and LCN2 in the *Ncstn*$^{flox/flox}$*;K5-Cre* mice increased compared with those in the WT mice at all four stages. Their protein expression levels similarly increased (Fig. 4B and 4D). Furthermore, both genes were upregulated on P0 compared with those of the WT mice. By contrast, the expression levels of *Tnf-α*, *Il23a*, and *Il1b*, which encode inflammatory cytokines upregulated in AI, did not increase on P0 (Fig. 2F–2H). Given that the upregulation of IL-36a is more significant than that of *Lcn2* on P0 and that IL-36a is also a novel inflammatory cytokine potentially involved in AI, we focused on IL-36a.

The tissue sections of the mouse skin were subjected to immunohistochemistry analysis. In the dermis of the mutant mice, the number of macrophages (as indicated by CD68) and dendritic cells (as indicated by CD11C) increased (Fig. 4E). In the damaged epidermis of these mice, Th17 cells, or possibly ILC3s (as indicated by RORγt), TNF-α, and IL-17A were found to be significantly higher than those in the skin of the WT mice (Fig. 4G–4H). Staining results also showed a significantly

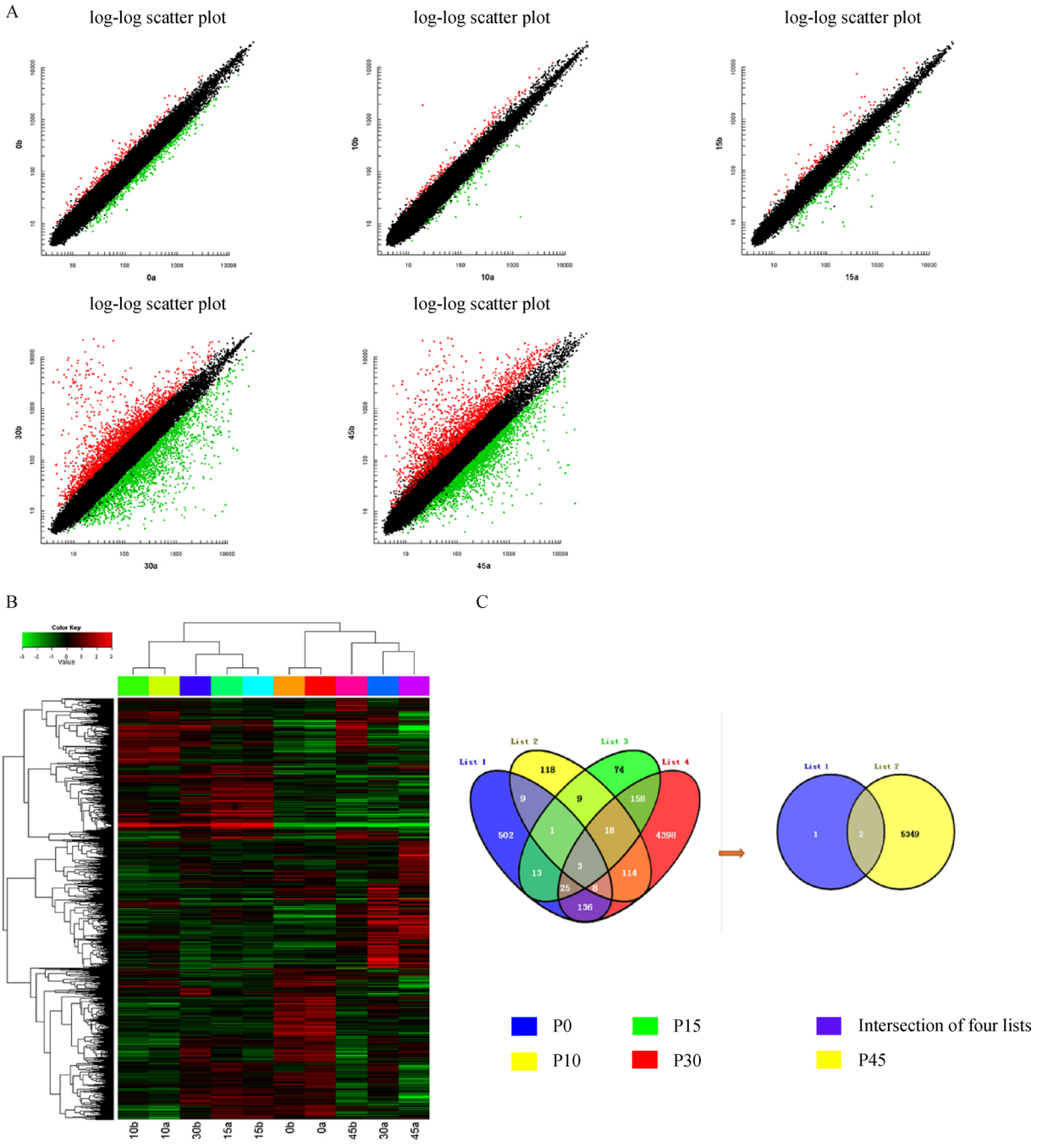

Fig. 3 Result of microarray analysis of *Ncstn*$^{flox/flox}$;*K5-Cre* mice. (A) The scatter plot on P0, P10, P15, P30, and P45 and (B) the hierarchical clustering map. (C) Three genes were screened from the intersection of four sets of data (P0, P10, P15, and P30) and intersected with the fifth set of data (P45), leaving only two differentially expressed genes.

higher IL-36a expression in the epidermis of the *Ncstn*$^{flox/flox}$;*K5-Cre* mice than in the WT mice. As indicated by the arrows in Fig. 4F, IL-36a was approximately colocalized with highly proliferated keratin 5-positive keratinocytes. Hence, our data implicated keratinocytes in the secretion of IL-36a, as described previously [34].

Increased *Sprr2d* expression in the skin of the AI mouse model

The entire transcriptome of the total skin tissue was assessed to determine the differential gene expression in the *Ncstn*$^{flox/flox}$;*K5-Cre* and WT mice on P0 and P30. The results of pairwise comparisons indicated a total of 3664

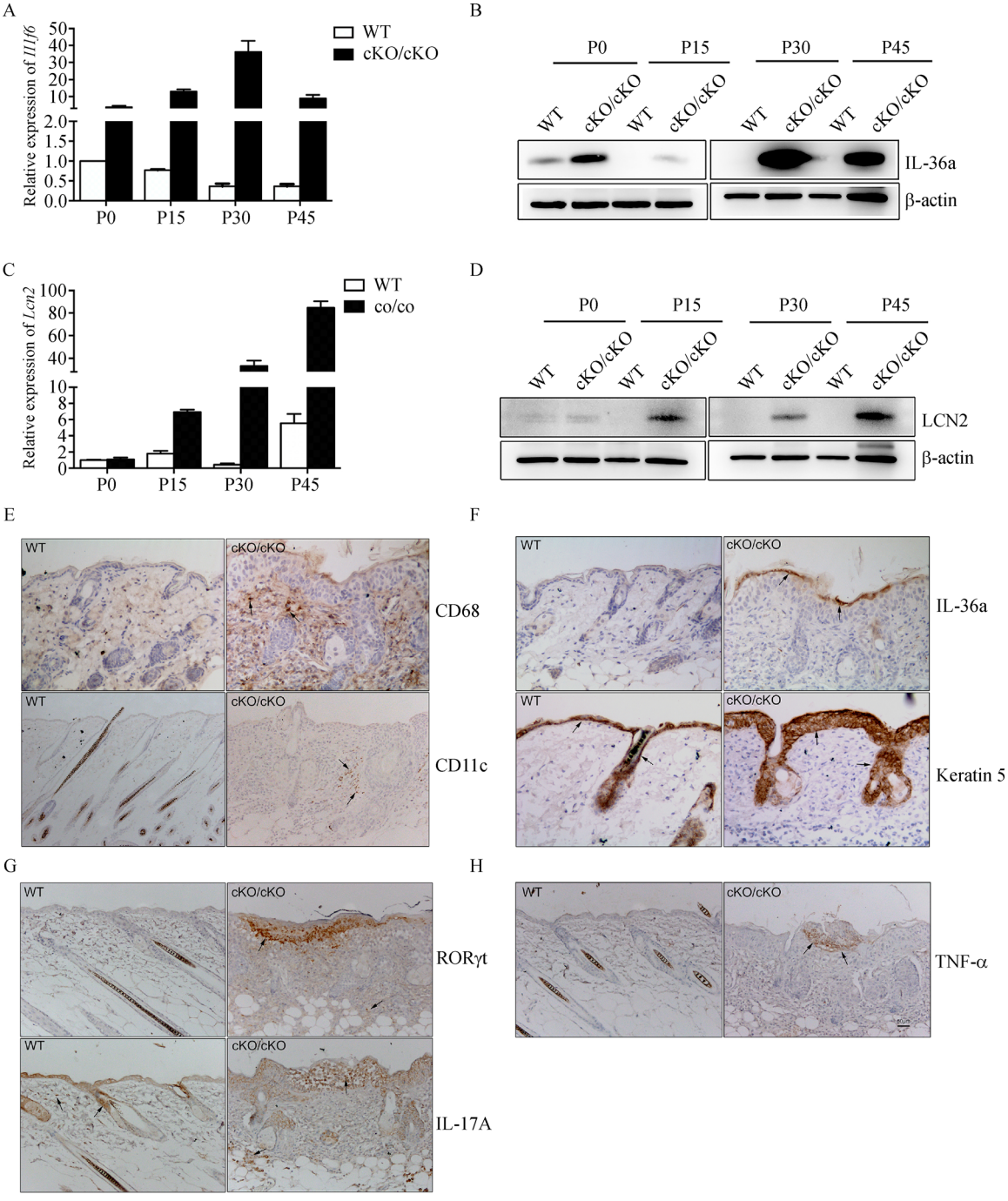

Fig. 4 Upregulation of IL-36a and LCN2 in the skin of the mouse model. Results of the quantitative reverse-transcription polymerase chain reaction and Western blot analysis of (A, B) IL-36a and (C, D) LCN2 expression in the skin of WT and *Ncstn*$^{flox/flox}$*;K5-Cre* mice on P0, P15, P30, and P45. Data shown were mean ± SD of three independent experiments, and each experiment was performed in duplicate. The ratio of the gene of interest to β-actin in WT mice on P0 was set to 1. Immunohistochemistry results for (E) CD68 (a marker of macrophages) and CD11c (a marker of dendritic cells), (F) IL-36a and keratin 5 (markers of keratinocytes), (G) RORγt (a marker of Th17 cells and ILC3) and IL-17A, and (H) TNF-α on P30 in the skin of WT and *Ncstn*$^{flox/flox}$*;K5-Cre* mice. Arrows specify the positively stained areas. Scale bar = 50 μm. The cKO/cKO group corresponded to *Ncstn*$^{flox/flox}$*;K5-Cre* mice.

upregulated and 3117 downregulated genes in the *Ncstn*$^{flox/flox}$;*K5-Cre* mice compared with those in the WT mice. The most enriched GO terms and Kyoto Encyclopedia of Genes and Genomes (KEGG) pathways were considered alongside the heat clustering map and volcano plot to ascertain the differentially expressed genes (Fig. 5). qRT-PCR was performed to validate the most relevant differentially expressed gene, namely, *Sprr2d*. The result showed that *Sprr2d* was significantly upregulated at multiple stages (P0, P15, P30, and P45; Fig. 6A). *Sprr* comprises a gene cluster that encodes small proline-rich proteins. As such, the expression levels of other *Sprr2* genes were also determined. Our results revealed that their expression levels also significantly increased (Fig. 6B–6D).

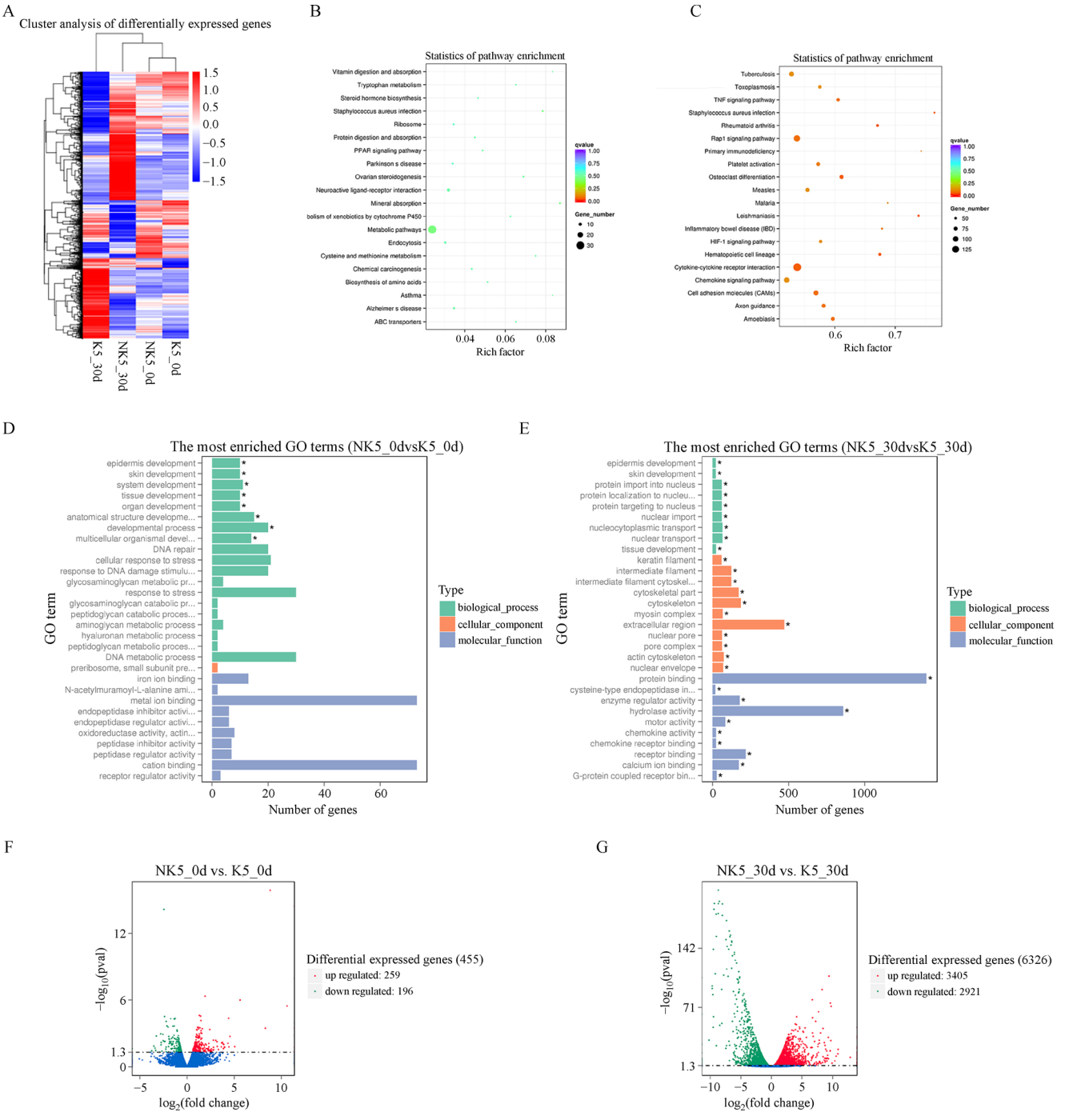

Fig. 5 RNA-seq analysis of *Ncstn*$^{flox/flox}$;*K5-Cre* mice versus K5-cre mice on P0 and P30. (A) Heat clustering map; (B,C) enriched pathways; (D,E) enriched gene ontology terms; and (F,G) volcano plot.

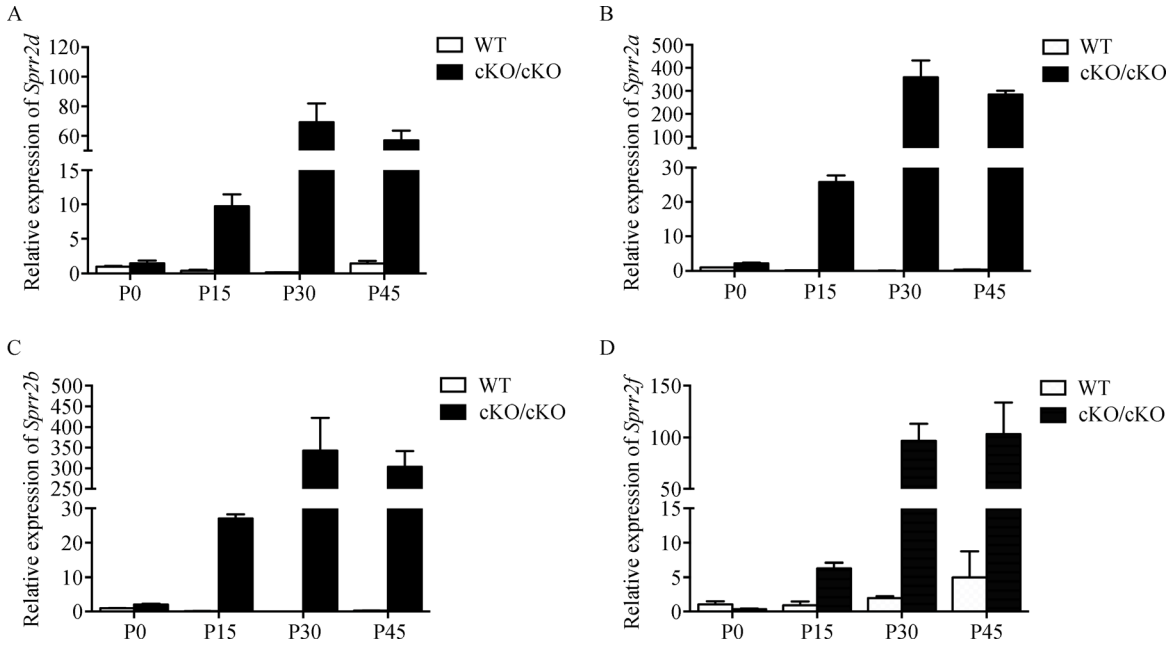

Fig. 6 Increased *Sprr2d* expression in the skin of the AI mouse model. The mRNA expression level of the *Sprr2* gene cluster in the skin of *Ncstn*$^{flox/flox}$*;K5-Cre* mice compared with that of WT mice at four stages (A–D). The ratio of the gene of interest to β-actin in WT mice on P0 was set to 1. Data shown were mean ± SD of three experiments, and each experiment was performed in duplicate. The cKO/cKO group corresponded to *Ncstn*$^{flox/flox}$*;K5-Cre* mice.

Upregulation of SPRR2 in *NCSTN*- and *NOTCH1*-downregulated HaCaT cells

We prepared HaCaT cells in which *NCSTN* and *NOTCH1* were downregulated by transfecting the cells with siRNAs targeting each of the two genes. We determined the knockdown efficiency of RNAi on NCSTN and Notch1 in terms of mRNA and protein expression levels. We found that the mRNA expression of NCSTN decreased by approximately 60%. The protein expression also reduced substantially in the cells transfected with NCSTN siRNA compared with that in the cells transfected with the negative control siRNA or a blank control (Fig. 7A and 7B). In *NOTCH1*-downregulated HaCaT cells, the knockdown efficiency of mRNA and protein expression was approximately 80% (Fig. 7D and 7E). As shown in Fig. 7C, Notch1 expression was lower in *NCSTN*-downregulated HaCaT cells than in negative control HaCaT cells. In HaCaT cells in which either NCSTN or Notch1 was downregulated, the expression levels of *SPRR2*-cluster genes increased (Fig. 7C and 7F). This finding was consistent with the results obtained from the mouse model. However, we did not detect significantly increased IL-36a and LCN2 expression levels in HaCaT cells transfected with NCSTN siRNAs (Fig. 7C). We observed a 2-fold increased IL-36a expression and an ~1.4-fold increased LCN2 expression in *NOTCH1*-downregulated cells (Fig. 7F).

Discussion

AI is a recurrent chronic inflammatory skin disease that primarily affects body parts rich in apocrine glands. The prevalence of AI ranges from 0.1% to 1% [2–5]. AI is characterized by painful nodules, abscesses, sinus tracts, and scarring; as such, this disease poses a major detriment to a patient's quality of life. Genetic factors are involved in the etiology of AI [6], and mutations in genes encoding the components of γ-secretase are consistently detected in patients with AI [35,36]. However, the pathogenesis of AI is not fully understood, and no appropriate animal AI model that recapitulates the disease phenotype has been established [37].

Herein, we established a keratin 5-Cre-driven epidermis-specific *Ncstn* conditional knockout mouse model of AI (*Ncstn*$^{flox/flox}$*;K5-Cre*). We validated this animal model experimentally by using whole skin specimens. This choice of tissue might explain why Ncstn expression was not totally abolished (Fig. 1D–1F). Additionally, the expression level of Ncstn did not correlate with the hair cycle. Therefore, the observed abnormal phenotypes in the mutant mice on approximately P30 were not related to the entry of the hair follicle into the first anagen phase.

The autosomal dominant inheritance pattern of familial AI is due to the haploinsufficiency of genes encoding γ-secretase subunits. However, our findings indicated that the heterozygous *Ncstn*$^{flox/+}$*;K5-Cre* mice showed no defect

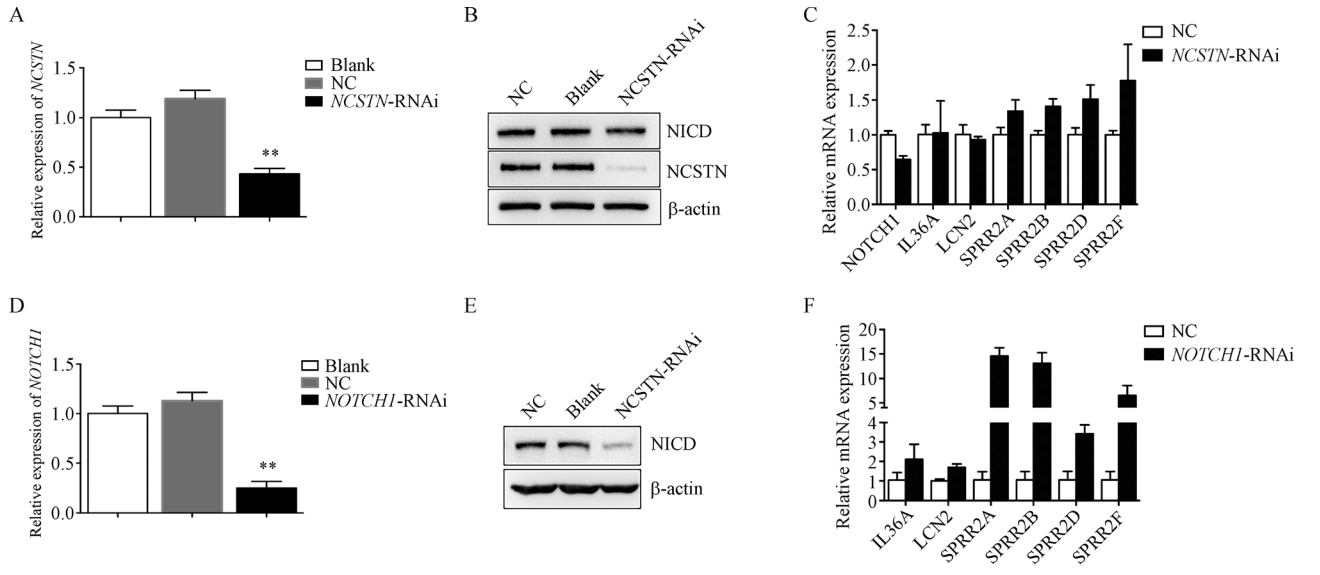

Fig. 7 Upregulation of SPRR2 in both *NCSTN*- and *NOTCH1*-downregulated HaCaT cells. siRNA-induced downregulation of (A, D) mRNA and (B, E) protein expression levels of *NCSTN* and *NOTCH1* was depicted in HaCaT cells. Two asterisks denoted $P < 0.01$. The ratio of the gene of interest to β-actin in the blank control was set to 1. The mRNA expression levels of IL-36a, LCN2, and SPRR2 were measured through quantitative reverse-transcription polymerase chain reaction in HaCaT cells in which (C) *NCSTN* or (F) *NOTCH1* was knocked down. The ratio of the gene of interest to β-actin in the negative control was set to 1. Data shown were mean ± SD of three experiments, and each experiment was performed in duplicate. NC, negative control. Blank, blank control.

possibly because Ncstn constituted only a conditional knockout in mice. In the *Ncstn*$^{flox/flox}$*;K5-Cre* mice, abnormal features emerged approximately on P21 and progressively worsened. The mutant mice exhibited key features of AI, including apparent keratinization, keratotic plug formation, and inflammation of the hair follicles (Fig. 2). However, some clinical features of AI, such as abscess, were absent in the mouse model. These differences were observed possibly because sweat glands are absent in mice and that mice and humans differ in terms of hair follicle cycles and hair distribution. Nevertheless, we posited that *Ncstn*$^{flox/flox}$*;K5-Cre* mice might be suitable for studying AI pathogenesis. To our knowledge, we were the first to establish a mouse AI model that recapitulated the clinical hallmarks of this disease.

AI is regarded as an autoinflammatory disorder [38] in which abundant inflammatory cytokines infiltrate skin lesions in affected patients. These cytokines include TNF-α, IL-1β, and IL-23A [22]. We found that these components were upregulated in the *Ncstn*$^{flox/flox}$*;K5-Cre* mice (Fig. 2). Our microarray data revealed that two genes, namely, *Lcn2* and *Il1f6*, were upregulated at all five stages. We verified these findings through qRT-PCR and Western blot in mice (Fig. 4A and 4D). LCN2 and IL-36a were upregulated in mutant mice on P0, whereas the other tested inflammatory cytokines were not upregulated. This finding indicated the potential role of IL-36a and LCN2 in the initiation of inflammation in AI.

We first addressed whether the IL-36a and LCN2 upregulation was directly related to the NCSTN or Notch1 downregulation. As shown in Fig. 7C and 7F, the IL-1F6 and LCN2 upregulation seemed to be associated with the *NOTCH1* downregulation. When the Notch1 expression was sufficiently high (i.e., approximately 80% of the NC), as in the *NCSTN*-knockdown cells (Fig. 7C), IL-36a and LCN2 were not significantly upregulated. In the *NOTCH1*-knockdown cells, the Notch1 expression was low (approximately 20% of NC), and IL-36a and LCN2 were both upregulated (Fig. 7F). Therefore, the IL-36a and LCN2 expression might be regulated directly by Notch1. We then validated our finding that IL-36a was upregulated on P0 in the *Ncstn*$^{flox/flox}$*;K5-Cre* mice, and this result was different from the clinical findings of other investigators [39,40]. Specifically, other authors determined that only patients suffering from AI and aged > 18 years have an increased IL-36a expression [41,42]. Accordingly, we speculated that IL-36a might play a role in the induction and exacerbation of inflammation in AI.

IL-36α is a recently described IL-1 family member that is expressed primarily in the skin and other epithelial tissues [43–45]. IL-36a binds to and signals through the IL1RL2/IL-36R receptor, which in turn activates NF-κB and MAPK signaling pathways in target cells to yield a proinflammatory response [46]. Some authors suggested that IL-36a may help regulate Th1 and Th17 immune responses [47], and Th17-driven autoinflammation participates in AI [38,48]. Other researchers confirmed the

prominent role of IL-36a in immune and inflammatory responses, especially in regulating inflammation in the skin [44]. Therefore, IL-36a, which is expressed at an early stage, can be implicated not only in regulating the expression of Th17 cells and enhancing their function but also in directly inducing the production of proinflammatory mediators (TNF-α, IL-6) that regulate the cellular and soluble components of the local inflammatory environment [44]. We speculated that IL-36a might act as a trigger in the pathogenesis of AI or at least function at the early stage of skin inflammation. Therefore, IL-36a might represent an important early target for the treatment of AI. Work is ongoing to better characterize the association of cytokines with keratinization.

For LCN2, other investigators suggested that LCN2 is highly correlated with TNF-α levels in patients with AI and can be used as a biomarker of AI disease activity [49]. This concept was supported by our results in mice and cells. The established mouse model in this study could be used to further address the role of LCN2 in the pathogenesis of AI.

We also detected the upregulation of the *Sprr2* genes in mutant mice (Fig. 6). The SPRR proteins are a set of structural proteins in the cornified cell envelope of most stratified squamous epithelia, and they provide barrier functions in epithelial cells [50]. The results of our *in vivo* and *in vitro* experiments (Fig. 4, and Fig. 5C and 5F) indicated the *Sprr2* upregulation, which corresponded to an impaired skin barrier. High *Sprr2* gene expression might explain the hyperkeratosis phenotype in patients with AI.

Nrf2 encodes a transcription factor that regulates genes via antioxidant response elements (AREs) in the promoter region. Many of the genes regulated by Nrf2 encode proteins involved in responses to injury and inflammation [51]. The Nrf2 upregulation in keratinocytes in mice upregulates cell-envelope proteins, such as Sprr2d, and exacerbates hyperkeratosis and inflammation [52]. Other studies have demonstrated that Notch1 possesses a functional ARE, and Nrf2 directly regulates the Notch1 expression in the mouse liver [53]. Conversely, the recruitment of the Notch intracellular domain to a conserved sequence in the promoter of *Nrf2* triggers Nrf2 activation and its stress-adaptive response pathway in the mouse liver [54]. Therefore, we speculated that a bidirectional Nrf2-Notch interaction, together with a Nrf2-Sprr2d interaction, might partly explain how *Ncstn* mutation yielded certain skin phenotypes in our mouse model and in patients with AI. Further investigations are needed to confirm whether the bidirectional interaction of Nrf2 and Notch occurred in the skin of our mouse model.

This study has some limitations. Primarily, this work described the histopathological findings of an AI-like mouse model and did not further explore underlying mechanisms, such as the regulation of IL36a and Sprr2 by Ncstn.

In summary, this study was the first to successfully establish a *K5*-specific *Ncstn* conditional knockout model in mice. We found that mice harboring mutant *Ncstn* had hyperkeratosis in hair follicles and inflammation, which recapitulated the major phenotypes of AI. An inflammatory factor (IL-36a) and a gene cluster with skin-barrier functions (Sprr2) significantly increased in this AI-like mouse model. We proposed that molecules of the skin barrier and some key inflammatory cytokines, including IL-36a (possibly the most important one), together with Sprr2, might contribute to the pathogenesis of AI.

Acknowledgements

This work was financially supported by the National Key Research and Development Program of China (No. 2016YFC0905100), the CAMS Innovation Fund for Medical Sciences (No. 2016-I2M-1-002), the National Natural Science Foundation of China (NSFC; Nos. 81788101 and 81230015), and the Beijing Municipal Science and Technology Commission (No. Z151100003915078) for Xue Zhang and by the National NSFC (No. 31271345) for Yaping Liu.

Compliance with ethics guidelines

Jun Yang, Lianqing Wang, Yingzhi Huang, Keqiang Liu, Chaoxia Lu, Nuo Si, Rongrong Wang, Yaping Liu, and Xue Zhang state no conflict of interest. All animal studies and procedures were approved by the Institutional Animal Care and Use Committee of Peking Union Medical College (Beijing, China).

Electronic Supplementary Material Supplementary material is available in the online version of this article at https://doi.org/10.1007/s11684-019-0722-8 and is accessible for authorized users.

References

1. Revuz J. Hidradenitis suppurativa. J Eur Acad Dermatol Venereol 2009; 23(9): 985–998
2. Garg A, Kirby JS, Lavian J, Lin G, Strunk A. Sex- and age-adjusted population analysis of prevalence estimates for hidradenitis suppurativa in the United States. JAMA Dermatol 2017; 153(8): 760–764
3. Revuz JE, Canoui-Poitrine F, Wolkenstein P, Viallette C, Gabison G, Pouget F, Poli F, Faye O, Roujeau JC, Bonnelye G, Grob JJ, Bastuji-Garin S. Prevalence and factors associated with hidradenitis suppurativa: results from two case-control studies. J Am Acad Dermatol 2008; 59(4): 596–601
4. Coughlan C, Ledger W, Wang Q, Liu F, Demirol A, Gurgan T, Cutting R, Ong K, Sallam H, Li TC. Recurrent implantation failure: definition and management. Reprod Biomed Online 2014; 28(1): 14–38
5. Jemec GB, Heidenheim M, Nielsen NH. The prevalence of hidradenitis suppurativa and its potential precursor lesions. J Am Acad Dermatol 1996; 35(2 Pt 1): 191–194
6. Ingram JR. The genetics of hidradenitis suppurativa. Dermatol Clin

2016; 34(1): 23–28
7. Schmitt JV, Bombonatto G, Martin M, Miot HA. Risk factors for hidradenitis suppurativa: a pilot study. An Bras Dermatol 2012; 87 (6): 936–938
8. Brook I, Frazier EH. Aerobic and anaerobic microbiology of axillary hidradenitis suppurativa. J Med Microbiol 1999; 48(1): 103–105
9. Jansen I, Altmeyer P, Piewig G. Acne inversa (alias hidradenitis suppurativa). J Eur Acad Dermatol Venereol 2001; 15(6): 532–540
10. Gao M, Wang PG, Cui Y, Yang S, Zhang YH, Lin D, Zhang KY, Liang YH, Sun LD, Yan KL, Xiao FL, Huang W, Zhang XJ. Inversa acne (hidradenitis suppurativa): a case report and identification of the locus at chromosome 1p21.1-1q25.3. J Invest Dermatol 2006; 126(6): 1302–1306
11. Von Der Werth JM, Williams HC, Raeburn JA. The clinical genetics of hidradenitis suppurativa revisited. Br J Dermatol 2015; 142: 947–953
12. Nomura Y, Nomura T, Suzuki S, Takeda M, Mizuno O, Ohguchi Y, Abe R, Murata Y, Shimizu H. A novel NCSTN mutation alone may be insufficient for the development of familial hidradenitis suppurativa. J Dermatol Sci 2014; 74(2): 180–182
13. Wang B, Yang W, Wen W, Sun J, Su B, Liu B, Ma D, Lv D, Wen Y, Qu T, Chen M, Sun M, Shen Y, Zhang X. γ-Secretase gene mutations in familial acne inversa. Science 2010; 330(6007): 1065
14. Kelleher RJ 3rd, Shen J. Genetics. γ-Secretase and human disease. Science 2010; 330(6007): 1055–1056
15. Prens E, Deckers I. Pathophysiology of hidradenitis suppurativa: an update. J Am Acad Dermatol 2015; 73(5 Suppl 1): S8–S11
16. Alikhan A, Lynch PJ, Eisen DB. Hidradenitis suppurativa: a comprehensive review. J Am Acad Dermatol 2009; 60(4): 539–561, quiz 562–563
17. Andersen RK, Jemec GB. Treatments for hidradenitis suppurativa. Clin Dermatol 2017; 35(2): 218–224
18. Giamarellos-Bourboulis EJ, Antonopoulou A, Petropoulou C, Mouktaroudi M, Spyridaki E, Baziaka F, Pelekanou A, Giamarellou H, Stavrianeas NG. Altered innate and adaptive immune responses in patients with hidradenitis suppurativa. Br J Dermatol 2007; 156 (1): 51–56
19. Chen Q, Bao H, Wu H, Zhao S, Huang S, Zhao F. Diagnosis of cobalamin C deficiency with renal abnormality from onset in a Chinese child by next generation sequencing: a case report. Exp Ther Med 2017; 14(4): 3637–3643
20. Sullivan TP, Welsh E, Kerdel FA, Burdick AE, Kirsner RS. Infliximab for hidradenitis suppurativa. Br J Dermatol 2003; 149(5): 1046–1049
21. Kurayev A, Ashkar H, Saraiya A, Gottlieb AB. Hidradenitis suppurativa: review of the pathogenesis and treatment. J Drugs Dermatol 2016; 15(8): 1017–1022
22. Kelly G, Hughes R, McGarry T, van den Born M, Adamzik K, Fitzgerald R, Lawlor C, Tobin AM, Sweeney CM, Kirby B. Dysregulated cytokine expression in lesional and nonlesional skin in hidradenitis suppurativa. Br J Dermatol 2015; 173(6): 1431–1439
23. Tong L, Corrales RM, Chen Z, Villarreal AL, De Paiva CS, Beuerman R, Li DQ, Pflugfelder SC. Expression and regulation of cornified envelope proteins in human corneal epithelium. Invest Ophthalmol Vis Sci 2006; 47(5): 1938–1946
24. Affymetrix. GeneChip® Expression Analysis. Data Analysis Fundamentals. 2004
25. Anders S, Huber W. Differential expression of RNA-Seq data at the gene level — the DESeq package. DESeq version 1.38.0. European Molecular Biology Laboratory (EMBL). 2013
26. Wang L, Feng Z, Wang X, Wang X, Zhang X. DEGseq: an R package for identifying differentially expressed genes from RNA-seq data. Bioinformatics 2010; 26(1): 136–138
27. Nomura Y, Nomura T, Suzuki S, Takeda M, Mizuno O, Ohguchi Y, Abe R, Murata Y, Shimizu H. A novel NCSTN mutation alone may be insufficient for the development of familial hidradenitis suppurativa. J Dermatol Sci 2014; 74(2): 180–182
28. Zhang X, Sisodia SS. Acne inversa caused by missense mutations in NCSTN is not fully compatible with impairments in Notch signaling. J Invest Dermatol 2015; 135(2): 618–620
29. Xiao X, He Y, Li C, Zhang X, Xu H, Wang B. Nicastrin mutations in familial acne inversa impact keratinocyte proliferation and differentiation through the Notch and phosphoinositide 3-kinase/AKT signalling pathways. Br J Dermatol 2016; 174(3): 522–532
30. Yang L, Mao C, Teng Y, Li W, Zhang J, Cheng X, Li X, Han X, Xia Z, Deng H, Yang X. Targeted disruption of Smad4 in mouse epidermis results in failure of hair follicle cycling and formation of skin tumors. Cancer Res 2005; 65(19): 8671–8678
31. Ramirez A, Page A, Gandarillas A, Zanet J, Pibre S, Vidal M, Tusell L, Genesca A, Whitaker DA, Melton DW, Jorcano JL. A keratin K5Cre transgenic line appropriate for tissue-specific or generalized Cre-mediated recombination. Genesis 2004; 39(1): 52–57
32. Wang B, Yang W, Wen W, Sun J, Su B, Liu B, Ma D, Lv D, Wen Y, Qu T, Chen M, Sun M, Shen Y, Zhang X. γ-Secretase gene mutations in familial acne inversa. Science 2010; 330(6007): 1065
33. Pink AE, Simpson MA, Desai N, Trembath RC, Barker JNW. γ-Secretase mutations in hidradenitis suppurativa: new insights into disease pathogenesis. J Invest Dermatol 2013; 133(3): 601–607
34. Boutet MA, Bart G, Penhoat M, Amiaud J, Brulin B, Charrier C, Morel F, Lecron JC, Rolli-Derkinderen M, Bourreille A, Vigne S, Gabay C, Palmer G, Le Goff B, Blanchard F. Distinct expression of interleukin (IL)-36α, β and γ, their antagonist IL-36Ra and IL-38 in psoriasis, rheumatoid arthritis and Crohn's disease. Clin Exp Immunol 2016; 184(2): 159–173
35. Pink AE, Simpson MA, Brice GW, Smith CH, Desai N, Mortimer PS, Barker JN, Trembath RC. PSENEN and NCSTN mutations in familial hidradenitis suppurativa (acne inversa). J Invest Dermatol 2011; 131(7): 1568–1570
36. Xu H, Xiao X, Hui Y, Zhang X, He Y, Li C, Wang B. Phenotype of 53 Chinese individuals with nicastrin gene mutations in association with familial hidradenitis suppurativa (acne inversa). Br J Dermatol 2016; 174(4): 927–929
37. van der Zee HH, Laman JD, Boer J, Prens EP. Hidradenitis suppurativa: viewpoint on clinical phenotyping, pathogenesis and novel treatments. Exp Dermatol 2012; 21(10): 735–739
38. van der Meer JW, Simon A. The challenge of autoinflammatory syndromes: with an emphasis on hyper-IgD syndrome. Rheumatology (Oxford) 2016; 55(suppl 2): ii23–ii29
39. Hessam S, Sand M, Gambichler T, Skrygan M, Rüddel I, Bechara FG. Interleukin-36 in hidradenitis suppurativa: evidence for a distinctive proinflammatory role and a key factor in the development of an inflammatory loop. Br J Dermatol 2018; 178(3): 761–767
40. Witte-Händel E, Wolk K, Tsaousi A, Irmer ML, Mößner R, Shomroni O, Lingner T, Witte K, Kunkel D, Salinas G, Jodl S,

Schmidt N, Sterry W, Volk HD, Giamarellos-Bourboulis EJ, Pokrywka A, Döcke WD, Schneider-Burrus S, Sabat R. The IL-1 pathway is hyperactive in hidradenitis suppurativa and contributes to skin infiltration and destruction. J Invest Dermatol 2019; 139(6): 1294–1305

41. Thomi R, Kakeda M, Yawalkar NSchlapbach C, Hunger RE. Increased expression of the interleukin-36 cytokines in lesions of hidradenitis suppurativa. J Eur Acad Dermatol Venereol 2017; 31 (12): 2091–2096
42. Di Caprio R, Balato A, Caiazzo G, Lembo S, Raimondo A, Fabbrocini G, Monfrecola G. IL-36 cytokines are increased in acne and hidradenitis suppurativa. Arch Dermatol Res 2017; 309(8): 673–678
43. Smith DE, Renshaw BR, Ketchem RR, Kubin M, Garka KE, Sims JE. Four new members expand the interleukin-1 superfamily. J Biol Chem 2000; 275(2): 1169–1175
44. Carrier Y, Ma HL, Ramon HE, Napierata L, Small C, O'Toole M, Young DA, Fouser LA, Nickerson-Nutter C, Collins M, Dunussi-Joannopoulos K, Medley QG. Inter-regulation of Th17 cytokines and the IL-36 cytokines *in vitro* and *in vivo*: implications in psoriasis pathogenesis. J Invest Dermatol 2011; 131(12): 2428–2437
45. Blumberg H, Dinh H, Trueblood ES, Pretorius J, Kugler D, Weng N, Kanaly ST, Towne JE, Willis CR, Kuechle MK, Sims JE, Peschon JJ. Opposing activities of two novel members of the IL-1 ligand family regulate skin inflammation. J Exp Med 2007; 204(11): 2603–2614
46. Towne JE, Garka KE, Renshaw BR, Virca GD, Sims JE. Interleukin (IL)-1F6, IL-1F8, and IL-1F9 signal through IL-1Rrp2 and IL-1RAcP to activate the pathway leading to NF-κB and MAPKs. J Biol Chem 2004; 279(14): 13677–13688
47. Vigne S, Palmer G, Martin P, Lamacchia C, Strebel D, Rodriguez E, Olleros ML, Vesin D, Garcia I, Ronchi F, Sallusto F, Sims JE, Gabay C. IL-36 signaling amplifies Th1 responses by enhancing proliferation and Th1 polarization of naive $CD4^+$ T cells. Blood 2012; 120(17): 3478–3487
48. Melnik BC, Plewig G. Impaired Notch-MKP-1 signalling in hidradenitis suppurativa: an approach to pathogenesis by evidence from translational biology. Exp Dermatol 2013; 22(3): 172–177
49. Wolk K, Wenzel J, Tsaousi A, Witte-Händel E, Babel N, Zelenak C, Volk HD, Sterry W, Schneider-Burrus S, Sabat R. Lipocalin-2 is expressed by activated granulocytes and keratinocytes in affected skin and reflects disease activity in acne inversa/hidradenitis suppurativa. Br J Dermatol 2017; 177(5): 1385–1393
50. Steinert PM, Candi E, Kartasova T, Marekov L. Small proline-rich proteins are cross-bridging proteins in the cornified cell envelopes of stratified squamous epithelia. J Struct Biol 1998; 122(1-2): 76–85
51. Wakabayashi N, Shin S, Slocum SL, Agoston ES, Wakabayashi J, Kwak MK, Misra V, Biswal S, Yamamoto M, Kensler TW. Regulation of notch1 signaling by nrf2: implications for tissue regeneration. Sci Signal 2010; 3(130): ra52
52. Schfer M, Farwanah H, Willrodt AH, Huebner AJ, Sandhoff K, Roop D, Hohl D, Bloch W, Werner S. Nrf2 links epidermal barrier function with antioxidant defense. EMBO Mol Med 2012(4): 364–379
53. Wakabayashi N, Chartoumpekis DV, Kensler TW. Crosstalk between Nrf2 and Notch signaling. Free Radic Biol Med 2015; 88 (Pt B): 158–167
54. Wakabayashi N, Skoko JJ, Chartoumpekis DV, Kimura S, Slocum SL, Noda K, Palliyaguru DL, Fujimuro M, Boley PA, Tanaka Y, Shigemura N, Biswal S, Yamamoto M, Kensler TW. Notch-Nrf2 axis: regulation of *Nrf2* gene expression and cytoprotection by Notch signaling. Mol Cell Biol 2014; 34(4): 653–663